

A New Four-Dimensional Hyperchaotic System with Four Unstable Equilibria: Dynamical Analysis, Bifurcation Structure, and Initial-Condition Sensitivity



Rana A. Sattar¹, Omar A. Jasim^{1*}, Dhuha M. Noori², Sadiq A. Mehdi³

¹ Ministry of Education, Baghdad Education Directorate (Rusafa First), Baghdad 10045, Iraq

² Ministry of Education, Baghdad Education Directorate (Al-Karkh Second), Baghdad 10011, Iraq

³ Department of Computer Science, College of Education, Mustansiriyah University, Baghdad 10052, Iraq

Corresponding Author Email: omar.abdul.ghafoor83@gmail.com

Copyright: ©2026 The authors. This article is published by IETA and is licensed under the CC BY 4.0 license (<http://creativecommons.org/licenses/by/4.0/>).

<https://doi.org/10.18280/ijss.160209>

ABSTRACT

Received: 8 December 2025

Revised: 31 January 2026

Accepted: 16 February 2026

Available online: 28 February 2026

Keywords:

four-dimensional hyperchaotic system, Lyapunov Exponent Spectrum, equilibrium points, bifurcation analysis, sensitivity to initial conditions, chaotic attractors, nonlinear dynamics

Hyperchaotic systems (HSs) have been of great interest due to their extreme complexity, nonlinear dynamics and possible importance in secure communication and information security. A new HS of four dimensions is suggested and discussed in this work. There are four equilibrium points (EPs) in the system and the spectrum of Lyapunov Exponents (LEs), as an indicator of hyperchaotic behavior, has two positive exponents, one zero exponent and one negative exponent over a large range of parameter values. The proposed model has a clear structural form as compared to the four-dimensional (4D) systems which had been reported before. Its dynamical properties are explored with phase portraits (PPs), bifurcation analysis, sensitivity to initial conditions (SDIC), and found to have a wide variety of nonlinear responses, which are complicated. The theoretical analysis and the numerical simulations support the obtained results. These features indicate that the proposed system can serve as a helpful foundation for future research in the field of secure communication, information security, and their application.

1. INTRODUCTION

With the emergence of chaos theory, cryptography has become more and more significant due to the unique characteristics that it displays, including randomness, extreme sensitivity to initial conditions (SDIC) and changes in parameters, periodicity, and mixing [1]. These characteristics have a strong interrelation with the principles of confusion and diffusion in cryptographic systems [2]. For this reason, Chaotic Systems (CSs) have been widely considered as a promising alternative to the conventional cryptographic methods [3].

CSs are a class of nonlinear dynamical models characterized by complex behavior and strong SDIC [4]. Throughout the last ten years, these systems have found extensive utility across diverse engineering disciplines, with a primary focus on secure communications and cryptographic applications [5]. Since the introduction of the three-dimensional Lorenz system in 1963 [6]. Numerous chaotic models with different structures and properties have been developed [7]. In chaos theory, designing systems with diverse dynamical behaviors and unique structures remains an important research direction [8]. Based on the characteristics of their basins of attraction, chaotic attractors can be classified as self-excited or hidden attractors [9]. In classical chaotic models, such as the Lorenz, Lü, and Chen systems, the attractors are typically self-excited [10]. Over the past few years, research on four-dimensional

hyperchaotic systems (4DHSs) has expanded significantly, including those derived from Chua, Chen, Lü, and Liu models [11]. Compared with the systems in lower dimensions, the systems in four dimensions generally have a greater dynamical complexity because of the presence of multiple Lyapunov Exponents (LEs) and a richer system behavior [12].

However, in spite of these developments, there are still a number of limitations in many reported 4DHSs [13]. Specifically, there are systems that are poorly suited to complex purposes because of a small equilibrium-point structure, a less multifaried distribution of LEs, or a simple dynamical structure [14].

This study presents a new model of hyperchaotic, a 4D model with a clear structural form with respect to the above-discussed limitations. The given model has four different states of equilibrium. Moreover, the spectrum of LE of the system always shows a piece of two positive, one null, and one negative exponent, which in a very large parameter space shows the system is complex. The properties imply much more interesting dynamical behaviour, as is shown by the phase portrait (PP), bifurcation, and sensitive dependence on initial conditions (ICs).

The remainder of this paper is organized as follows: Section 3 is the review of the related literature, Section 4 talks about the suggested system, Section 5 investigates its dynamical characteristics, and Section 6 is the summary of the key results.

2. SURVEY OF RELEVANT LITERATURE

Several 4DHSs have been introduced in previous studies, with varying structural forms and dynamical characteristics. These systems differ greatly in terms of parameter number, EP configurations, LE distributions, and intended applications.

In 2024, Ozpolat et al. [15] proposed a new 4DHS and conducted an in-depth dynamical analysis. Their paper analyzed the system in the form of bifurcation diagrams, Lyapunov exponents, PPs, sensitivity to initial conditions, Kaplan-Yorke dimension, symmetry analysis. The results reported corroborated the existence of hyperchaotic behavior, having two positive LEs ($L1 = 4.742, L2 = 0.061, L3 = 0, L4 = -45.046$) and a Kaplan-Yorke Dimension (KYD) of about 3.106. Besides, circuit simulation was used to check the physical feasibility of the system and the model was also extended to synchronization and image encryption.

In 2023, Shahna [16] proposed 4D hyperchaotic Lorenz-based image encryption. The model uses four control parameters and produces hyperchaotic behaviour with the existence of multiple positive LEs. Its main focus is application, especially in encryption, where permutation and substitution methods using keystreams are implemented to increase the security level.

In 2022, Al-Azzawi and Al-Hayali [17] proposed a four-dimensional hyperchaotic extension of the Sprott-S model in 2022. Their study demonstrated that the system possesses a single EP and can generate both self-excited and hidden coexisting attractors. The reported model also exhibits multistability, as different attractors may arise for the same parameter values under different ICs. Additionally, having two positive LEs establishes the hyper-chaotic nature of the system, all while keeping a comparatively straightforward two-parameter framework.

In a 2022 study, Dong and Wang [18] presented a novel 4DHS defined by five control parameters alongside two EPs. They found that they were hyperchaotic, as was evidenced by the Lyapunov Exponent Spectrum (LES) and the Kaplan-Yorke dimension of about 3.0696. Although the reported model exhibits complex dynamics, its equilibrium-point structure and LE distribution remain relatively limited compared with some more recent hyperchaotic systems (HSs).

In a 2021, Mehdi [19] new 4DHS was developed utilizing eight control parameters. Its strong hyperchaotic nature was established through a KYD of nearly 3.12998 alongside two positive LEs. However, the model is characterized by attractive dynamical properties, although its parametric complexity is relatively large, thus making the structure of the model not as compact as the simpler 4DHSs.

In 2021, Shakir et al. [20] introduced another 4DHS involving ten parameters and strong sensitivity to ICs. The hyperchaotic behavior of the reported model was verified by its LES, together with a KYD of approximately 3.069890. Nevertheless, the relatively large number of parameters may increase the complexity of the system and diminish its applicability in the real world.

In 2018, Ababneh [8] proposed a four-dimensional chaotic system (4DCS) that has two control parameters and a relatively straightforward structure. The model has a unique positive LE, a sign of chaotic, as opposed to hyperchaotic behavior, and a Kaplan-Yorke dimension of approximately 1.6296. Although the system has the advantage of structural simplicity, the dynamical richness is less than higher-complexity four-dimensional hyperchaotic models.

Based on the above review, it is clear that several four-dimensional systems that were previously reported entailed a trade-off between simplicity and dynamical performance. Generally, simple systems, which are structurally simple, are expected to have less diverse dynamics. Conversely, a system where a nonlinear potential exists is said to have more parameters or more limiting equilibrium-point properties.

In these regards, the proposed system will aim to offer a better balance between the two aspects. It is characterized by a medium parameter space, two (or more) EPs, and a LES that contains two positive exponents, thus exhibiting apparent hyperchaotic dynamics.

Accordingly, the proposed model can be regarded as offering a richer dynamical response than several earlier systems summarized in Table 1, while retaining a structure that remains sufficiently manageable for further analysis. Possible practical implementation and application-oriented investigation may be considered in future studies.

3. SYSTEM DESIGN

In the present work, a novel 4DHS is developed. The resulting autonomous framework is mathematically defined by the following set of nonlinear differential systems:

$$\begin{aligned} \frac{dx}{dt} &= -ax - czw + y(bz - d \cos(w)) \\ \frac{dy}{dt} &= -y - x(z - ew + zw) \\ \frac{dz}{dt} &= -fz - x(y + w - yw) \\ \frac{dw}{dt} &= x(gy + z) + y(hz - i \cos(w)) \end{aligned} \quad (1)$$

Let $x, y, z,$ and w be the dynamic state variables evolving over time $t \in R$. The system's behavior is governed by a set of positive real parameters. Throughout this research, we utilize the following specific configuration for these coefficients:

$$(a, b, c, d, e, f, g, h, i) = (24, 20, 5, 10, 3.1, 2.5, 26, 0.8, 9).$$

Additionally, the simulations are initialized starting from

$$(x(0), y(0), z(0), w(0)) = (2.5, 1, 1.5, 2)$$

Under these settings, the system exhibits hyperchaotic behavior. Unless stated otherwise, the same parameter set is used throughout the subsequent analysis.

All numerical simulations and PPs were generated using Mathematica software.

3.1 Dynamical analysis of the proposed system

Unless otherwise specified, all theoretical and simulation-based results in this subsection are obtained by using the parameter set and initial states introduced in Section 3.

This subsection is devoted to the study of system (1) from several dynamical viewpoints, including its EPs, LES, attractor behavior, and fractal dimension. These investigations provide a comprehensive description of the model behavior

under the adopted parameter setting.

The Fourth-Order Runge–Kutta (RK4) algorithm was employed to perform all numerical simulations, utilizing a constant time step size of $\Delta t = 0.01$.

The time taken for simulation was decided to allow the system trajectories to converge. To remove short term effects, a small part of the data was cut off prior to plotting the results. The values of the parameters used in each of the analyses are indicated in the individual figures.

In the bifurcation analysis, (f) was added and (z) was the consecutive local maxima of the state variable, and parameter, (f) lied between [2.1, 2.3].

3.1.1 Analysis of equilibrium points and stability

By equating the time derivatives to zero, the EPs of system (1) can be evaluated, which yields the subsequent algebraic equations:

$$\begin{aligned} 0 &= -ax - czw + y(bz - d \cos(w)) \\ 0 &= -y - x(z - ew + zw) \\ 0 &= -fz - x(y + w - yw) \\ 0 &= x(gy + z) + y(hz - i \cos(w)) \end{aligned} \quad (2)$$

$$[(a, b, c, d, e, f, g, h, i) = (24, 20, 5, 10, 3.1, 2.5, 26, 0.8, 9)]$$

system (1) has four distinct equilibrium points (EPs):

$$E_0 = (0, 0, 0, 0),$$

$$E_1 = (-88.4477, -209607, 6337.86, 37282.3),$$

$$E_2 = (-9.27867, -0.448162, 6337.86, 2.69692),$$

$$E_3 = (-6.9433, 0.288421, -7.10834, -3.31497).$$

For system (1), the corresponding Jacobian matrix (J) is expressed in the form:

$$[J = \frac{\partial F}{\partial X}]$$

with the state vector given by $X = (x, y, z, w)^T$ and the vector field denoted by $F = (f_1, f_2, f_3, f_4)^T$.

To analyze the nature of the stability of the equilibrium states, the J is first determined of the given point. We then get the necessary Eigenvalues (EVs) indirectly by the characteristic equation:

$$[\det(\lambda I - J) = 0] \quad (3)$$

To obtain the main EP, which is determined by ($E_0 = (0, 0, 0, 0)$), the resulting EVs are determined to be:

$$[\lambda_1 = -24, \quad \lambda_2 = -2.5, \quad \lambda_3 = -1, \quad \lambda_4 = 0].$$

Because one of the EVs is zero with the others being negative, then the EP (E_0) is unstable and non-hyperbolic.

Similarly, the remaining EPs (E_1), (E_2), and (E_3) are also found to be unstable under the same parameter values.

3.2 Dissipativity analysis

System (1) can be concisely expressed in a vector representation as follows:

$$\dot{X} = F(X),$$

where, the state variables form the vector $X = (x, y, z, w)^T$. The divergence associated with this vector field (F) is formulated as:

$$[\nabla \cdot F = \frac{\partial f_1}{\partial x} + \frac{\partial f_2}{\partial y} + \frac{\partial f_3}{\partial z} + \frac{\partial f_4}{\partial w}]$$

Substituting the expressions of system (1) yields:

$$[\nabla \cdot F = -a - 1 - f] \quad (4)$$

For the selected parameter values ($a = 24$) and ($f = 2.5$), we obtain:

$$[\nabla \cdot F = -27.5 < 0]$$

According to Liouville's theorem, the time evolution of a volume ($V(t)$) in the phase space is given by:

$$[\frac{dV}{dt} = (\nabla \cdot F)V(t)]$$

Thus,

$$[\frac{dV}{dt} = -27.5 V(t)]$$

Solving this differential equation leads to:

$$V(t) = V(0)e^{-27.5t} \quad (5)$$

Since ($\nabla \cdot F < 0$), the system is dissipative, and every trajectory is eventually closed in a confined part of the phase space.

3.3 Symmetry analysis

System (1) has the remarkable aspect of structural invariance with regard to the transformation:

$$[(x \mapsto -x), (y \mapsto -y), (z \mapsto -z), (w \mapsto -w)] \quad (6)$$

This is the symmetry that can be checked by replacing the transformed variables in system (1), keeping the equations the same.

Thus, the system will be symmetrical along the (z) – (w) plane. This property may lead to the existence of symmetric attractors and is responsible, among other things, for the richness of the system's dynamical behaviour.

3.4 Spectrum of Lyapunov exponents and Kaplan–Yorke dimension

The computation of the Les is crucial to the dynamical character of any nonlinear system and its sensitivity to Ics. Utilizing the parameter configuration specified earlier in Section 3, the computed exponents for system (1) yield the following values:

$$[(L_1, L_2, L_3, L_4) = (1.95247, 1.05247, 0, -22.6213).]$$

Because two of these calculated exponents hold positive values, it is firmly established that the system operates within a hyperchaotic regime. Furthermore, to approximate the attractor's fractal dimension, the Kaplan–Yorke (or Lyapunov) dimension is utilized, which is formulated mathematically as:

$$[D_{KY} = j + \frac{\sum_{i=1}^j L_i}{|L_{j+1}|}] \quad (7)$$

where, (j) is the maximum integer for which the following condition holds:

$$[\sum_{i=1}^j L_i > 0 \quad \text{and} \quad \sum_{i=1}^{j+1} L_i < 0]$$

In this case ($j = 3$), since:

$$[L_1 + L_2 + L_3 > 0, \quad \text{and} \quad L_1 + L_2 + L_3 + L_4 < 0]$$

Based on the above relation, the Kaplan–Yorke is determined as:

$$[D_{KY} = 3 + \frac{1.95247 + 1.05247 + 0}{22.6213} \approx 3.13284]$$

These results suggest that the system is characterized by a fractal structure and rich hyperchaotic dynamics.

3.5 Phase portraits analysis

Phase diagrams of the system (5) are depicted in Figures 1-8, with the parameter values provided in Section 3 and the numerical model set up in Section 4.

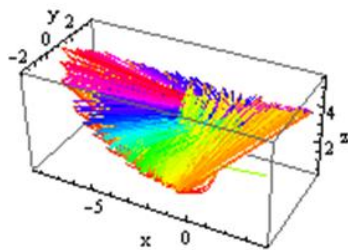


Figure 1. 3-D phase portraits (PPs) of system (5) in the (x, y, z) phase-space, highlighting the geometric structure of the attractor

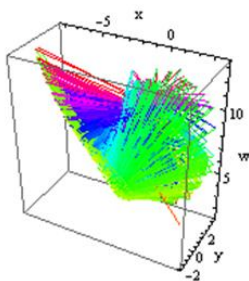


Figure 2. 3-D representation of the phase trajectory of system (5) in the (x, y, w) phase space, illustrating the attractor geometry

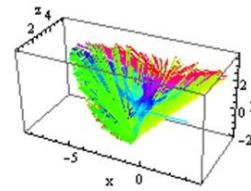


Figure 3. 3-D representation of the phase trajectory of system (5) in the (x, z, y) phase space, illustrating the attractor geometry

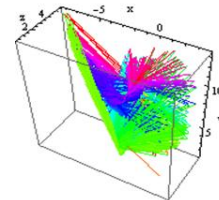


Figure 4. 3-D representation of the phase trajectory of system (5) in the (x, z, w) phase space, illustrating the attractor geometry

Figures 1-4 display three-dimensional projections of the system trajectories across various phase spaces, providing a clear visualization of the attractor's geometric structure. These projections show that we have a complex and bounded attractor meaning that this system is dissipative.

In Figures 5 through 8, two-dimensional phase plane projections are presented to highlight distinct non-linear and aperiodic trajectory patterns within the model. The highly complex, interwoven nature of these paths serves as strong evidence for both the sensitivity of the system to ICs and its unpredictable state evolution. Ultimately, evaluating both the 2D and 3D projections collectively reveals the intricate dynamic properties of the introduced model, substantiating its hyperchaotic nature.

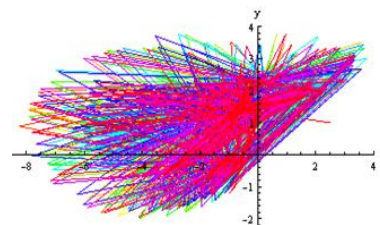


Figure 5. 2-D projection of the phase trajectory of system (5) in the (x, y) phase space, showing the aperiodic evolution of the trajectories

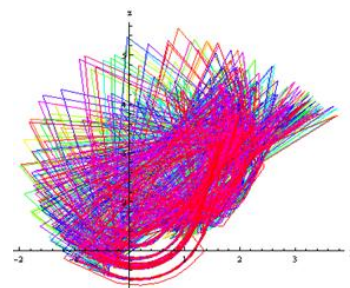


Figure 6. 2-D projection of the phase trajectory of system (5) in the (z, y) plane, showing the aperiodic evolution of the trajectories

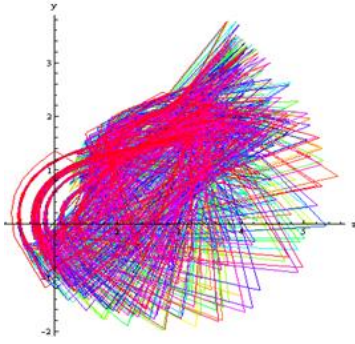


Figure 7. 2-D projection of the phase trajectory of system (5) in the (y, z) plane, showing the aperiodic evolution of the trajectories

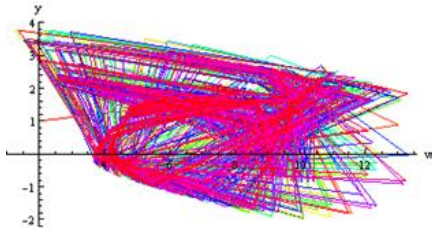


Figure 8. 2-D projection of the phase trajectory of system (5) in the (y, w) plane, showing the aperiodic evolution of the trajectories

Time-Domain Analysis of the Proposed System

Fundamentally, hyperchaotic models are defined by highly irregular and non-periodic behaviors within the time domain. By analyzing these time-domain responses, the intricate dynamical traits of the proposed system are clearly demonstrated. Consequently, Figures 9-12 plot the curves of the $x(t)$, $y(t)$, $z(t)$, and $w(t)$ of state variables, which were generated according to the precise numerical settings in Section 4 and the specific parameters detailed in Section 3.

Figure 9 shows the time evolution of $x(t)$ which has irregularities but no periodic repetition. Figure 10 shows the behavior of $y(t)$, which confirms the aperiodic behavior of the system response. Figure 11 shows the time evolution of $z(t)$, in which nonlinear oscillations are clearly observed. More complex temporal behavior appears in Figure 12, which presents the response of $w(t)$.

Overall, the irregular and non-periodic behavior of all the state variables confirms the complex hyperchaotic behavior exhibited by the developed system.

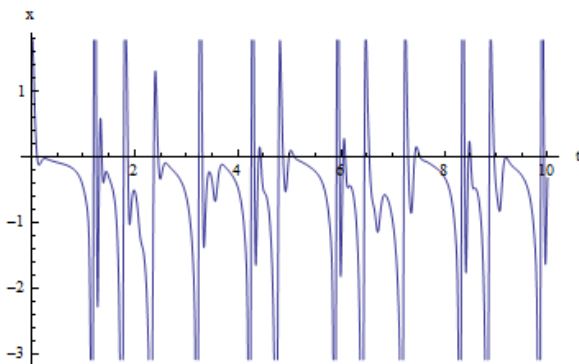


Figure 9. Time domain response of the state variable $(x(t))$ of the proposed system, showing irregular and non-periodic behavior

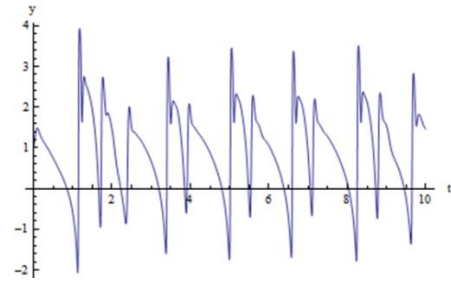


Figure 10. Time domain response of the state variable $(y(t))$ of the proposed hyperchaotic system, illustrating the aperiodic evolution of the system dynamics

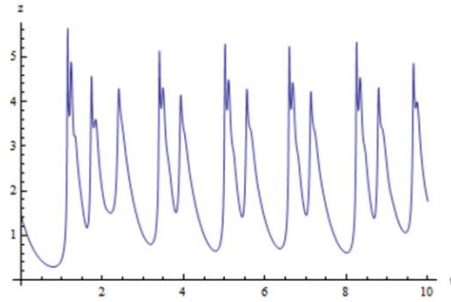


Figure 11. Time domain response of the state variable $(z(t))$ of the proposed system, demonstrating nonlinear and irregular oscillations

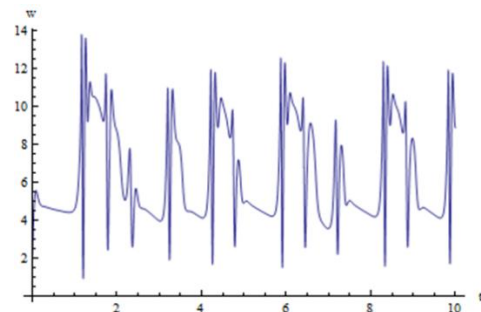


Figure 12. Time domain response of the state variable $(w(t))$ of the proposed system, highlighting the complex temporal behavior of the system

3.6 Sensitivity of system dynamics to initial states

SDIC in HSs, ICs in the system are a fundamental quality of a CSs, where if the ICs are slightly varied, the resulting trajectories will be significantly different over time.

In order to illustrate this property, two sets of ICs are considered. The first set is given by:

$$[(x_0, y_0, z_0, w_0) = (2.5, 1, 1.5, 2).]$$

To observe the rapid divergence of trajectories, a second, minutely altered starting point is selected where only the third variable is slightly modified:

$$[(x_0, y_0, z_0, w_0) = (2.5, 1, 1.5000000000000001, 2)].$$

The evolution of time for the corresponding is shown in Figures 13-16. The divergence in $(x(t))$ is shown in Figure 13, divergence in $(y(t))$ is shown in Figure 14, behaviour of $(z(t))$ shown in Figure 15 and response of $(w(t))$ shown in

Figure 16. In all cases, while the starting conditions are almost identical, the trajectories branch out in a very short time.

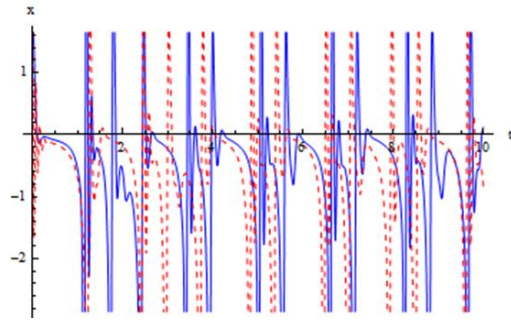


Figure 13. Sensitivity analysis of the proposed system for the state variable ($x(t)$) using two nearby initial conditions, showing rapid divergence of trajectories

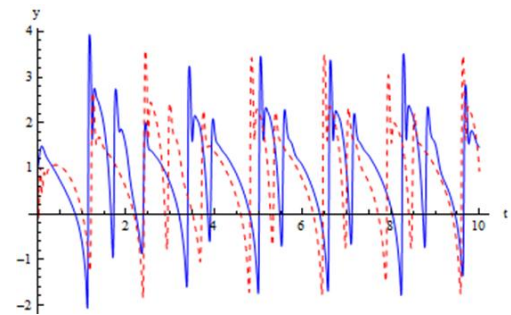


Figure 14. Sensitivity analysis of a proposed system with respect to the state variable ($y(t)$), showing the divergence of trajectories with respect to small variations in the initial conditions

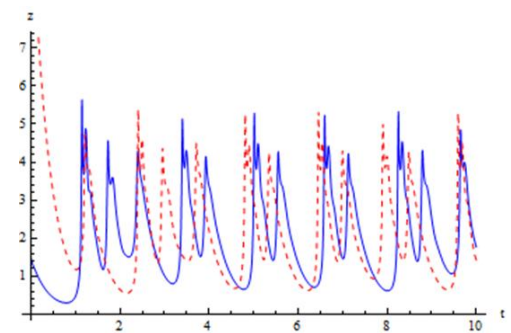


Figure 15. Sensitivity investigation for the proposed system for the state variable ($z(t)$), demonstrating strong sensitivity to initial conditions (SDIC)

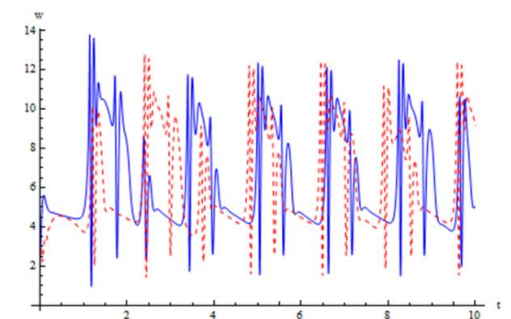


Figure 16. Sensitivity study of the proposed system regarding the state variable ($w(t)$) under consideration, and the rapid separation of paths with time

This rapid onset of divergence demonstrates the high level of sensitivity to ICs and the existence of hyperchaotic nature of the proposed system.

3.7 Bifurcation diagram analysis

To thoroughly investigate the system's dynamical behavior across a range of values for parameter (f), a corresponding Bifurcation Diagram (BD) was generated. The number-wise simulations were run with the setups mentioned above in Section 4. The last step was to eliminate the initial transient responses and plot the calculated local maxima of the state variable z to get the most final BD, and this is shown in Figure 17.

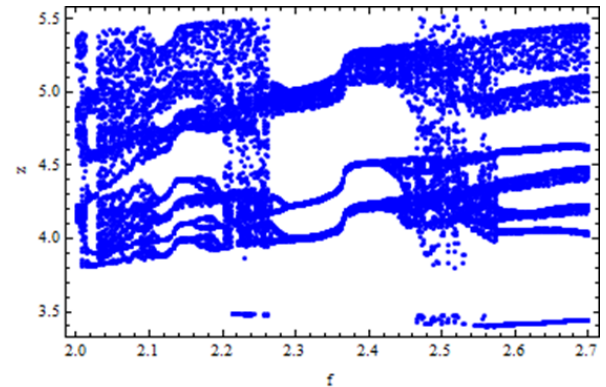


Figure 17. Bifurcation diagram of the proposed system as a function of parameter (f), which shows the evolution from a periodic regime to a complex and chaotic regime through a series of bifurcations

As the parameter f changes in the interval $[2.1, 2.3]$, a series of bifurcations, including period-doubling transitions, occur in the system, and more and more complicated dynamics of the system is obtained. One of the pieces of evidence that there can be chaotic dynamics is the high concentration of points in a certain area.

These results eventually highlight the extremely intricate dynamical character of the new system, which precisely corresponds to the HS formulated in the previous sections.

4. DYNAMICAL ANALYSIS AND PERFORMANCE ASSESSMENT OF THE NEW MODEL

There is a comparative analysis that enables a validation of the performance of the proposed HS and contrasts the main dynamic characteristics of the system in relation to the models of the previous literature, as outlined in Table 1. Dual positive Lyapunov-exponents is the ultimate evidence of hyperchaotic, indicating a superior level of complex behaviour in comparison to other 4D systems. Moreover, the analysis of the Kaplan-Yorke dimension supports this intricacy, as there is a very rich and fractal dynamical structure.

Structurally, the system is constructed using a comparatively simple set of nonlinearities, and it is nevertheless able to produce complicated hyperchaotic behaviour. This simplicity of structure and richness of dynamics is quite conducive to the analysis and potential implementation.

Also, there is a flexible structure of controlling system behavior through use of parameters, where parameter

adjustment possibilities are involved, which is not an excessively complex structure when compared to some of the existing models.

In summary, the proposed system is a balanced solution in terms of the complexity of the dynamics and simplicity of the

structure. All these qualities qualify it to be used in engineering in the future, whilst the job of practical application and demonstration of performance is under further development.

Table 1. Comparison between the new four-dimensional system and the performance of the previously documented chaotic and hyperchaotic models

Characteristics	Proposed	Ref. [15]	Ref. [16]	Ref. [17]	Ref. [18]	Ref. [19]	Ref. [20]
Lyapunov exponents	1.95247	4.742	Multiple	0.2041	0.7796	1.09792	4.05761
	1.05247	0.061	positive	0.0023	0.1058	2.9891	0.347562
	0	0	Lyapunov	-0.0008	0	-1.99733	-3.94257
	-22.6213	-45.046	exponents	-1.2056	-12.7177	-16.0776	-6.61896
DKY	3.13284	3.106	Not reported	3.1705	3.0696	3.12998	3.069890
No. of Parameters	9	2	4	2	5	8	10
Key Characteristics	4D hyperchaotic model featuring dual positive Lyapunov exponents alongside four completely unstable equilibria.	4D hyperchaotic system with two control parameters, dual positive Lyapunov exponents, circuit implementation, and image-encryption application.	4D Lorenz-based hyperchaotic image-encryption model with four control parameters and multiple positive Lyapunov exponents.	4D hyperchaotic system with one equilibrium point (EP), multistability, and coexisting self-excited/hidden attractors.	4D hyperchaotic framework possessing two EPs and dual positive Lyapunov exponents.	4D hyperchaotic structure governed by a single EP and two positive Lyapunov exponents.	4D hyperchaotic demonstrating a single positive Lyapunov exponent.

Table 1 to show that the proposed system is a good balance of dynamical complexity and structural simplicity. The proposed system has a richer dynamical behavior but a flexible and controllable structure as compared to systems with fewer parameters or just one EP. This balance helps in studying analytically and implementation, thus the system is more appropriate in practical applications in engineering.

5. CONCLUSION

This study introduces and investigates a novel 4D nonlinear dynamical model. The presence of hyperchaotic within the proposed architecture is confirmed by the derivation of dual positive LEs, specifically $L_1 \approx 1.95247$ and $L_2 \approx 1.05247$. Consequently, these metrics firmly demonstrate the system's profound dynamic complexity and its acute dependence on starting states.

The equilibrium analysis reveals that the system possesses four EPs, all of which are unstable. Furthermore, the KYD is approximately 3.13284, reflecting the fractal nature and high dynamical complexity of the attractor.

To thoroughly evaluate the behavioral characteristics of the system, multiple analytical methods were applied, encompassing Bifurcation Diagrams (BDs), PPs, evaluations of Initial Condition Sensitivity (ICS), and time-domain responses. These comprehensive assessments reveal that the newly introduced model possesses highly diverse and complex dynamic traits.

The system could be a possible foundation to the further engineering applications, especially in the area of the secure communication and other conditions. The next steps in work are on practical implementation and further validation of work

on the real world.

DECLARATIONS

Data Accessibility

This research does not rely on any outside datasets. Instead, the findings are derived exclusively from the mathematical derivations and computational experiments detailed throughout the paper.

Use of Artificial Intelligence (AI) Tools Statement

The authors certify that the scientific core, including data analysis and primary findings, was developed without the involvement of artificial intelligence. AI-based tools were strictly limited to enhancing linguistic clarity and grammatical accuracy. Every part of the work has been meticulously scrutinized by the authors, who maintain absolute accountability for the integrity of the final paper.

CONFLICT OF INTEREST DISCLOSURE

No competing financial or personal interests that could influence the work reported in this manuscript are declared by the authors.

The book size should be in A4 (8.27 inches × 11.69 inches). Do not change the current page settings when you use the template.

The number of pages for the manuscript must be no more than ten, including all the sections. Please make sure that the whole text ends on an even page. Please do not insert page numbers. Please do not use the Headers or the Footers because

REFERENCES

[1] El Den, A.M.M., Moussa, K.H., Zaki, A., Khedr, M.E. (2025). An Enhanced Pseudorandom Number Generator Based on 5D-Memrestive Hyperchaotic Map. In 2025 International Telecommunications Conference (ITC-Egypt), pp. 213-218. <https://doi.org/10.1109/ITC-Egypt66095.2025.11186646>

[2] Taha, M.D., Hussein, K.A. (2023). Generation S-box and P-layer For PRESENT algorithm based on 6D hyper chaotic system. *Al-Kitab Journal for Pure Sciences*, 7(01): 48-56. <https://doi.org/10.32441/kjps.07.01.p5>

[3] Mehdi, S.A., Jabbar, K.K., Abbood, F.H. (2018). Image encryption based on the novel 5D hyper-chaotic system via improved AES algorithm. *International Journal of Civil Engineering and Technology*, 9(10): 1841-1855. https://iaeme.com/Home/article_id/IJCIET_09_10_183.

[4] Jasim, O.A., Amer, S.R., Hussein, S.F., Mehdi, S.A. (2024). Enhanced image encryption using a novel chaotic system and scramble dithering technique. *International Journal of Safety & Security Engineering*, 14(5): 1465-1476. <https://doi.org/10.18280/ijss.140514>

[5] Hussein, K.A., Mahmood, S.A., Abbass, M.A. (2019). A new permutation-substitution scheme based on Henon chaotic map for image encryption. In 2019 2nd Scientific Conference of Computer Sciences (SCCS), pp. 63-68. <https://doi.org/10.1109/SCCS.2019.8852590>

[6] Jasim, O.A., Hussein, K.A. (2021). A hyper-chaotic system and adaptive substitution box (S-Box) for image encryption. In 2021 International Conference on Advanced Computer Applications (ACA), pp. 144-149. <https://doi.org/10.1109/ACA52198.2021.9626793>

[7] Lin, H., Wang, C., Yu, F., Sun, J., Du, S., Deng, Z., Deng, Q. (2023). A review of chaotic systems based on memristive Hopfield neural networks. *Mathematics*, 11(6): 1369. <https://doi.org/10.3390/math11061369>

[8] Ababneh, M. (2018). A new four-dimensional chaotic attractor. *Ain Shams Engineering Journal*, 9(4): 1849-1854. <https://doi.org/10.1016/j.asej.2016.08.020>

[9] Das, P., Singh, P.P. (2021). A 4D chaotic system with seventeen equilibria: Synchronization and anti-synchronization. In 2021 1st International Conference on Power Electronics and Energy (ICPEE), pp. 1-6. <https://doi.org/10.1109/ICPEE50452.2021.9358496>

[10] Hussein, K.A., Mahmood, S.A. (2019). A parallel programming for robust chaotic map generation based on two dimensional equation system. *Journal of Engineering and Applied Sciences*, 14(11): 3741-3745. <https://makhillpublications.co/public/view-article/1816-949x/jeasci.2019.3741.3745>.

[11] Rashid, A.A., Hussein, K.A. (2023). A lightweight image encryption algorithm based on elliptic curves and a 5D logistic map. *Iraqi Journal of Science*, 5985-6000. <https://doi.org/10.24996/ijs.2023.64.11.41>

[12] Shakir, H.R., Mehdi, S.A.A., Hattab, A.A. (2022). Chaotic-DNA system for efficient image encryption. *Bulletin of Electrical Engineering and Informatics*,

11(5): 2645-2656. <https://doi.org/10.11591/eei.v11i5.3886>

[13] Cui, N., Li, J. (2023). A new 4D hyperchaotic system and its control. *Aims Math*, 8(1): 905-923. <https://doi.org/10.3934/math.2023044>

[14] Ali, F., Jhangeer, A., Muddassar, M. (2025). Comprehensive classification of multistability and Lyapunov exponent with multiple dynamics of nonlinear Schrödinger equation. *Nonlinear Dynamics*, 113(9): 10335-10364. <https://doi.org/10.1007/s11071-024-10781-x>

[15] Ozpolat, E., Celik, V., Gulten, A. (2024). A novel four-dimensional hyperchaotic system: Design, dynamic analysis, synchronization, and image encryption. *IEEE Access*, 12: 126063-126073. <https://doi.org/10.1109/ACCESS.2024.3454820>

[16] Shahna, K.U. (2023). Novel chaos based cryptosystem using four-dimensional hyper chaotic map with efficient permutation and substitution techniques. *Chaos, Solitons & Fractals*, 170: 113383. <https://doi.org/10.1016/j.chaos.2023.113383>

[17] Al-Azzawi, S.F., Al-Hayali, M.A. (2022). Coexisting of self-excited and hidden attractors in a new 4D hyperchaotic Sprott-S system with a single equilibrium point. *Archives of Control Sciences*, p. 32. <https://doi.org/10.24425/acs.2022.140863>

[18] Dong, C., Wang, J. (2022). Hidden and coexisting attractors in a novel 4D hyperchaotic system with no equilibrium point. *Fractal and Fractional*, 6(6): 306. <https://doi.org/10.3390/fractalfract6060306>

[19] Mehdi, S.A. (2021). Image encryption algorithm based on a novel 4D chaotic system. *International Journal of Information Security and Privacy (IJISP)*, 15(4): 118-131. <https://doi.org/10.4018/IJISP.2021100107>

[20] Shakir, H.R., Mehdi, S.A., Hattab, A.A. (2023). A new four-dimensional hyper-chaotic system for image encryption. *International Journal of Electrical and Computer Engineering*, 13(2): 1744-1756. <https://doi.org/10.11591/ijece.v13i2.pp1744-1756>

NOMENCLATURE

4D	Four-Dimensional
4DHS	Four-Dimensional Hyperchaotic System
HS	Hyperchaotic System
4DCS	Four-Dimensional Chaotic System
CS	Chaotic System
LE	Lyapunov Exponent
LES	Lyapunov Exponent Spectrum
KYD	Kaplan–Yorke Dimension
EP	Equilibrium Point
RK4	Fourth-Order Runge–Kutta
J	Jacobian Matrix
EVs	Eigenvalues
ICS	Initial Condition Sensitivity
SDIC	Sensitivity to Initial Conditions
BD	Bifurcation Diagram
ICs	Initial Conditions